JOURNAL OF APPLIED ELECTROCHEMISTRY **28** (1998) 663–672

A printed circuit board approach to measuring current distribution in a fuel cell

S. J. C. CLEGHORN, C. R. DEROUIN, M. S. WILSON, S. GOTTESFELD

Material Science and Technology Division, MS D429, Los Alamos National Laboratory, Los Alamos, NM 87545, USA

Received 25 June 1997; revised 3 November 1997

A new method of measuring current distribution in a polymer electrolyte fuel cell of active area 100 cm^2 has been demonstrated, using a printed circuit board (PCB) technology to segment the current collector and flow field. The PCB technique was demonstrated to be an effective approach to fabricating a segmented electrode and provide a useful tool for analysing cell performance at different reactant gas flow rates and humidification strategies. In this initial chapter of work with the segmented cell, we describe measured effects on current distribution of cathode and anode gas stream humidification levels in a hydrogen/air cell, utilizing a Nafion^{TM} 117 membrane and single serpentine channel flow fields, and operating at relatively high gas flow rates. Effects of the stoichiometric flow of air are also shown. A clear trend is seen, apparently typical for a thick ionomeric membrane, of lowering in membrane resistance down the flow channel, bringing about the highest local current density near the air outlet. This trend is reversed at low stoichiometric flows of air. At an air flow rate less than three times stoichiometry, the local performance starts to drop significantly from inlet to outlet, as local oxygen concentration drop overshadows the lowering in resistance along the direction of flow.

Keywords: *fuel cell*, *segmented electrode*, *current distribution*, *water distribution*

1. Introduction

Within the last several years activities worldwide on polymer electrolyte fuel cell (PEFC) technology for both transportation and stationary power applications have flourished, to a large extent as a result of key advances like decreased catalyst loadings and improved fuel cell membranes. PEFC researchers and potential manufacturers are currently developing fuel cell stacks and integrated fuel processor/PEFC power systems. Scaling up PEFC stacks could present challenges in efficient utilization of active electrode area, as the size of electrodes increases to accommodate larger stack power and dimensions.

At Los Alamos, a number of stack designs are being considered based on a number of different types of flow fields, all evaluated first in a 100 cm^2 active area polymer electrolyte (single) fuel cell. To achieve efficient scale-up to higher active area, the design of the gas flow field is critical. It is expected that it would be more difficult to provide optimal reactant, water and temperature distribution over the area of larger cells, resulting in nonuniform current distribution. Poor current distribution in the PEFC could result in poor reactant and catalyst utilization, reduced energy efficiency, and, possibly, corrosion processes in the cell. In general, current distribution is a function of the local concentration of electroactive species at the electrode surface, as well as the potential distribution in the cell [1].

A number of methods of measuring current distribution in electrolytic cells have been reported, these include incorporating arrays of micro or mini electrodes into the electrode of interest [2] or segmenting the electrode either by the machining of insulated electrode blocks [3] or using a printed circuit board technology [4, 5]. Measurement of current distribution has recently been reported for a PEFC with a circular active electrode area and flow channels arranged in pie shaped sections [6]. In this latter experiment, the current collector flow field was partitioned and then bonded back together into its original configuration with insulating material separating each segment. Several authors have mathematically modelled water and temperature distribution in PEFCs. These efforts included modelling of the water profile across the thickness of the membrane [7, 8], and of water and temperature profiles along the length of the flow channel [9, 10]. Models have shown that local current densities could be highly dependent upon these (interrelated) variables down a simple single flow channel. Nguyen *et al*. [9] chose to study current distribution at high current densities for three different anode humidification strategies and dry cathode feed. The poor current distribution observed suggested that back diffusion of water from cathode to anode was insufficient under the cell conditions used to maintain a uniformly humidified membrane. The less severe fuel cell operating conditions assumed by Fuller *et al*. [10]

0021-891X

resulted in more uniform current distributions. At moderate humidified air flow rates, water diffusion back to the anode was sufficient to provide higher current densities as distance from the cathode inlet increased.

In this work, we have adapted the printed circuit board approach to measure the current distribution in a polymer electrolyte fuel cell. This method was previously reported [5] for characterizing current distribution in the ICI FM01 laboratory electrolyser cell (with active electrode area of 64 cm^2). As far as we are aware, this technology has not previously been exploited to measure current distributions in fuel cells other than a preliminary report by these authors [11]. The PCB technology approach may provide a number of advantages over the previous method reported [6], including the relatively cheap and rapid manufacture of a wide range of segment patterns [5].

To minimize perturbation of the measured system by the structural changes required to perform current distribution measurements, we decided to not perturb, in the first segmented cell fabricated, the cathode flow field/current collector. Instead, we chose to segment the anode side of the fuel cell, given the facile nature of the hydrogen oxidation reaction. Therefore, any perturbation made in the anode structure by segmentation should not too strongly affect cell performance. Each anode segment can thus be seen as a probe for monitoring local cathode activity and local membrane conductivity. PEFC cathode performance is determined by oxygen reduction kinetics and oxygen transport to catalyst sites [12, 13]. Both processes depend upon local water activity/content: sufficient water must be present to provide efficient oxygen reduction reaction catalysis, however excess liquid water acts as a barrier to oxygen access to catalyst sites. It is the function of the cathode structure and flow field to effectively supply oxygen and manage water to maintain uniformly high cell performance. The local resistance of the membrane reflects, at least to first approximation, local water content [7]. Distribution of membrane resistance along the flow channels was measured in this work by following variations in segment high frequency resistance. In this initial chapter of work with our segmented cell, we tried to demonstrate the ability of a specific cell design and fabrication, described in detail in the Experimental section below, to effectively probe current distribution in a PEFC along the flow channel and indicate how it varies with some cell operation parameters. We preferred to use for these first viability tests an ionomeric membrane (Nafion^{TM} 117), cell flow fields (seven parallel serpentine channels) and cell operation conditions which facilitated initial fabrication and testing. We examined first humidification conditions and air stoichiometric flow effects on current distribution, under relatively high fuel flow rates. Next to each experiment described below, we comment on the domain of relevance of the observations made by us, considering the specific components and specific operation conditions employed. Full technological relevance of such diagnostic experiments obviously depends on a specific cell/stack design and specific operation conditions. This paper attempts to present a new, effective diagnostic tool, rather than define generalized technological conclusions.

2. Experimental details

2.1. *Cell configuration*

The fuel cell design used for current distribution measurements was based on the 100 cm^2 hardware previously reported by Los Alamos [14], that incorporated seven channel serpentine flow fields on both anode and cathode sides of the cell. A typical single cell (described in [14]) consisted of air and hydrogen stainless steel current collectors with seven machined channel serpentine flow fields, separated by a membrane electrode assembly (MEA). The cell was sealed using silicone gaskets on each side of the MEA.

To investigate the current distribution in this cell, the anode side of the cell was segmented. This required segmentation of the anode catalyst layer, the anode gas diffusion backing and the current collector/hydrogen gas flow field. The cell configuration containing a segmented anode and PCB current collector/flow field is shown in Fig. 1. The anode current collector plate/flow field consisted of a PCB with a seven channel serpentine flow field machined into it (see Fig. 2). A PCB with isolated copper segments in the desired configuration was first fabricated, the copper segments were then gold plated (to provide good corrosion resistance) and the serpentine flow field pattern was machined into this board. The resulting gas flow field contained 18 gold plated segments which acted as electrically isolated current collectors (each current collector segment had an area of 4.4 cm^2). Each segment was designed to cover approximately half a pass across the plate of the seven parallel channels of the serpentine flow field. (The seven channels of the flow field make a total of nine passes across the plate from inlet to outlet). Gold plated-through holes linked the top side of the board to the underside, where two current traces connected

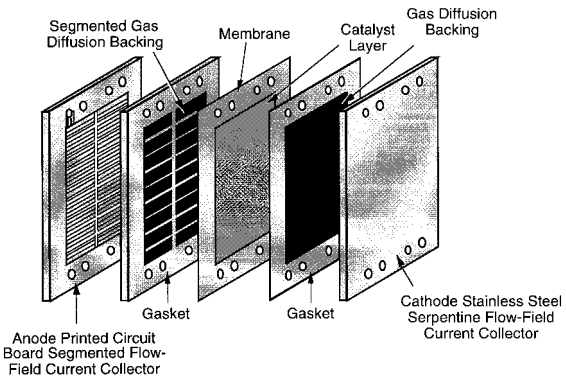

Fig. 1. Unit cell configuration for fuel cell containing the segmented anode.

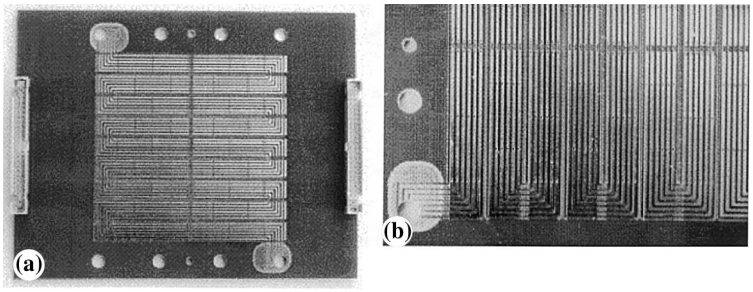

Fig. 2. Photograph of the printed circuit board segmented electrode with the seven channel serpentine flow field current collector used on the anode side of the cell (a) and a close-up of the printed circuit board (b) showing flow channels.

each segment to the fuel cell test equipment (Figure 3). One line was used as a voltage sense and the other to carry current.

The gas diffusion backing (E-Tek, Natick, MA. carbon cloth) was segmented by cutting silicone gasket material into a grid structure, with the cut-out areas filled with gas diffusion backing to match the pattern of the gold plated segments of the current collector plate (see Fig. 4). The MEA consisted of a catalysed Nafion^{TM} 117 membrane (DuPont), prepared using a catalyst ink and the 'decal' method of catalyst application to the membrane [15]. The ink used contained 5% Nafion^{TM} solution (1100 equiv. wt. from Solution Technologies, Mendenhall, PA), 20% platinum on carbon (Vulcan XC-72, E-Tek) and a number of different solvents. Anode and cathode catalyst layers were prepared with loadings of 0.14 mg Pt cm^{-2}. The anode catalyst layer was segmented by etching the 18 segment pattern into the dried catalyst ink with a knife while on the Teflon blank [15], followed by hot pressing onto the membrane. In this way each segment of the anode half cell was completely electrically isolated from its neighbours.

2.2. *Experimentation*

Reactant humidification, gas flow rates, back pressure, and fuel cell temperature were all controlled from a fuel cell test station. The gas flow rates have been measured at room temperature and ambient pressure, which at Los Alamos (elevation 2300 m) is 0.77 atm. The temperatures quoted for cathode and for anode humidifiers in each experiment described below, are the nominal humidifier (internal) thermocouple readings. Actual measured gas humidification levels were 70% ($\pm$ 5%) of the saturated water vapour pressure corresponding to each nominal temperature reported. (Gas stream humidification efficiency fell below 100% when gas reactant flows were increased to accommodate a cell of 100 cm^2 active area, as a result of limited residence time in the humidifier liquid).

For cell operation, the 18 current lines from the anode current collector plate were connected to a primary electronic load box (Hewlett-Packard 6050A electronic load box) outside the cell at a specially designed patch board. The load box was operated in constant voltage mode and was regulated by a voltage sense from one of the segments. The choice of sense position was found to have negligible effect upon the measured current distribution. In the experiments described the voltage of the 17 segments was controlled by using segment 3, and segment 1 was used for voltage sense when segment 3 was isolated for investigation.

To monitor the current of the individual segments (i.e. current distribution) in the cell, each of the 18 segments was uncoupled in turn from the other 17 on the patch board and the voltage sense and current line from the uncoupled segment were then connected to a second load box. A schematic of the electronics hardware is shown in Fig. 5. This allowed the performance of this isolated single segment in the cell to be measured separately. The isolated segment and the other 17 segments comprising the cell were maintained at the same voltage versus the cathode using the two load boxes. Therefore, as the performance of one segment was monitored, the remainder of the cell

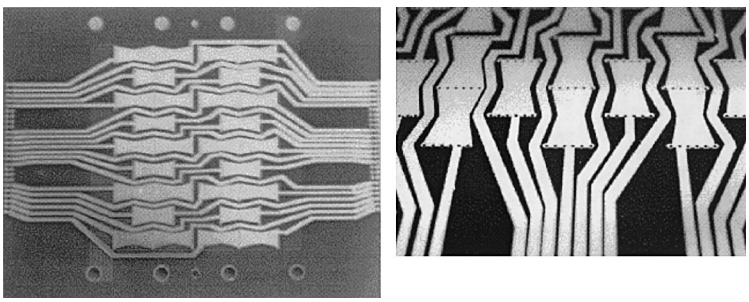

Fig. 3. Photograph of the reverse side (a) and close-up (b) of the printed circuit board segmented electrode showing the current and voltage sense lines fed from the eighteen segments to the edges of the board.

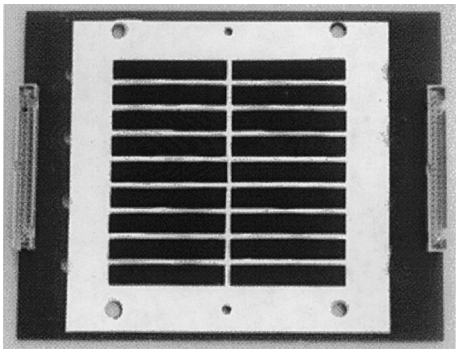

Fig. 4. Photograph of the segmented gas diffusion backing and gasket.

was operating under normal conditions, that is, the performance of a single region of the cell could be investigated while the consumption of reactants and the generation or uptake of water throughout the cell was the same as that expected while the cell is operated ordinarily.

The load boxes were both interfaced to a Macintosh (Apple) computer so that polarization curves and/or high frequency resistance measurements of individual segments or the entire cell could be made, using programs written with Labview (National Instruments) software. High frequency resistance was measured at 8 kHz with a signal magnitude of 0.04 V peak to peak using a Solartron SI 1260 frequency response analyser.

Cell operating conditions were varied significantly to determine what effect cathode and anode humidification conditions, as well as cathode flow rate (air stoichiometry) would have on the current distribution in the cell. The results for current distribution are plotted such that air inlet is at segment number 1 (see Fig. 6). The segment numbering system then follows the path of air along the serpentine flow field channels from 1 to 2 to 3 etc. to the air outlet at segment number 18. Hydrogen inlet (on the opposite side of the membrane) is at segment number 2 and flows counter to air (i.e., segment number 2 to 1 to 3 to 4 etc., see Fig. 6). No data was obtained for segment number 16 due to a problem in the electrical circuitry.

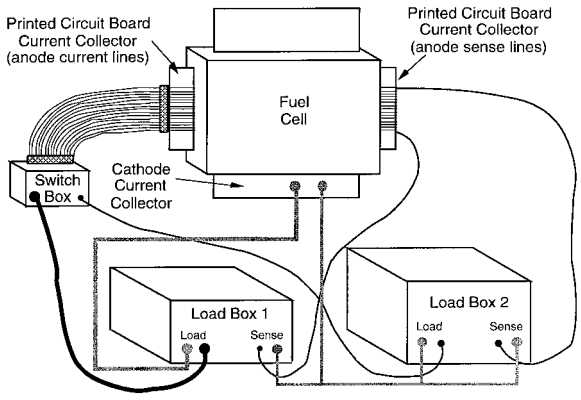

Fig. 5. Schematic diagram of the electronics hardware to measure current distribution in the fuel cell.

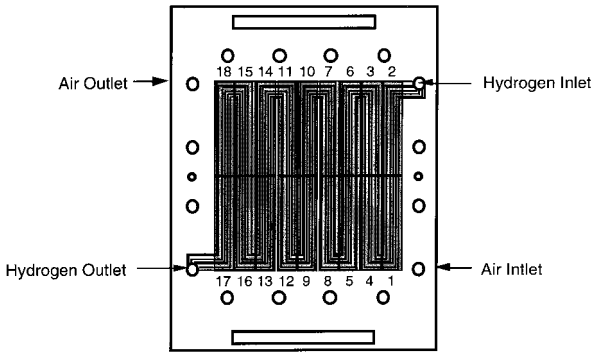

Fig. 6. Schematic representation of the front side of the printed circuit board. The lines represent the gas flow channels and the shaded areas the isolated gold segment current collector plates. This was used as the anode current collector plate and flow field. The air inlet was at segment number 1 and outlet at number 18. The segment numbering system follows the path of air flow along the path of the gas flow field. The hydrogen (on the opposite side of the membrane) inlet is at segment number 2 and flows in the counter direction to air (i.e., segment number 2 to 1 etc.).

3. Results and discussion

Current and high frequency resistance distribution measured for the cell (Fig. 7) based on a Nafion^{TM} 117 membrane and operated at 80 °C, with hydrogen at 700 ml min^{-1}, humidified at nominal 100 °C and pressurized to 2.8 atm and air at 5.0 l min^{-1}, humidified at nominal 80 °C and pressurized to 2.8 atm are shown for three operating voltages, 0.7, 0.5 and 0.2 V. These flows of both hydrogen and air are very high (low utilization of both). Individual segment currents show some fabrication dependent variations in current from segment to segment. These appear as some 'noise' superimposed on any trend detected along the flow channel. A number of general explanations can be considered to account for these variations in performance of individual segments in the cell: differences in interfacial contact between catalyst layer, gas diffusion backing and current collector, blockage in the gas flow channel of the serpentine flow field by the backing protruding in the gas channels or by condensate and variability of catalyst layer performance. The current 'noise' is relatively small at 0.7 V (segment current density between 0.17 and 0.27 A cm^{-2}), however as the cell current increases at 0.5 V (0.50 and 0.73 A cm^{-2}) it increases and at 0.2 V (0.63 to 0.95 A cm^{-2}), there is a larger variation of segment performance within the cell. The variability seems to be a similar fraction of the average current at each voltage.

The current distributions along the flow channels at all three voltages show a similar trend. Proceeding from air inlet down the flow channel the segment performance decreases to a minimum (around segment number 6) before increasing to the highest values near the air outlet. These features are most evident at the lowest operating voltage (highest current density). This behaviour is an indication that the cathode catalyst layer and/or the membrane are insufficiently well humidified near the air inlet. A similar trend in current distribution was predicted by the

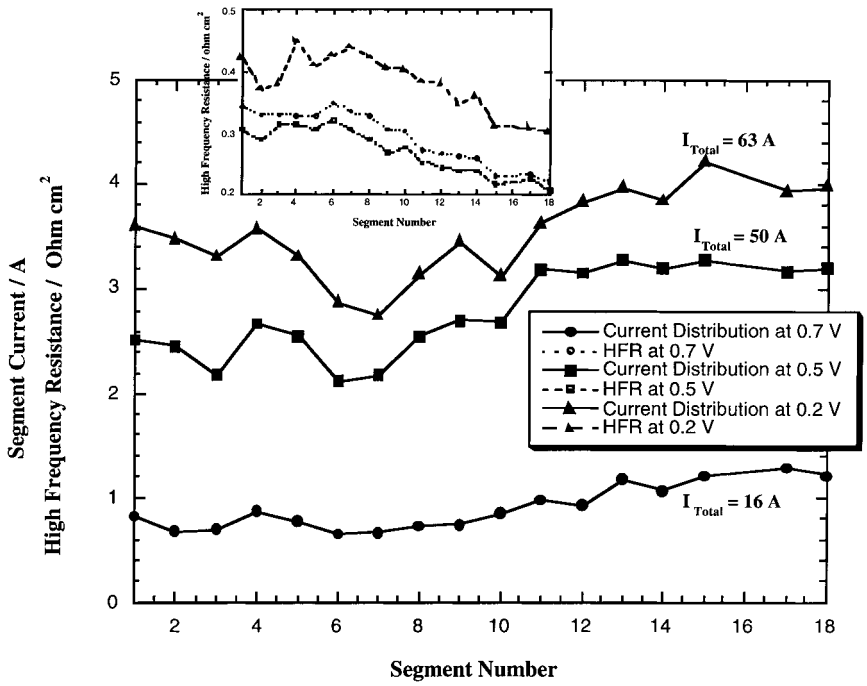

Fig. 7. Current and high frequency resistance distribution for a hydrogen/air cell with a Nafion^{TM} 117 membrane, operated at 80 °C at cell voltages 0.7, 0.5 and 0.2 V. Hydrogen was humidified at 100 °C and passed through the cell at 0.7 l min^{-1}, at a back pressure of 2.8 atm. Air was humidified at 80 °C and passed through the cell at 5.0 l min^{-1}, at a back pressure of 2.8 atm. (Temperatures quoted for cathode and for anode humidifiers are nominal humidifier (internal) thermocouple readings; actual measured gas humidification levels were 70% (± 5%) of the saturated water vapour pressure corresponding to each nominal temperature.)

model of Fuller *et al.* [10], although cell conditions were different and the trend was predicted over a much smaller channel length. A high flow of less than fully humidified air was the probable reason for the low activity of segments near air inlet. With the air humidification level only 70% of vapour saturation level at cell temperature (see Experimental), the high air flow would have a drying effect near the inlet. The increase in segment performance further down the flow field (i.e., beyond segment 8 in our experiments) is explained by internal humidification of the MEA, by water generated at the cathode. This internally generated water humidifies the air stream as it passes through the cell and thus increases the water content in the membrane in contact with the air down stream. Increased water content in the air stream provides sufficient water to generate water diffusion back to the anode, counter acting electroosmotic drag and hence reducing the net flux of water through the membrane away from the anode [7]. As a consequence, the anode side of the membrane remains better humidified even at high current densities. This results in better local performance the further the distance from air inlet.

High frequency resistance (HFR) distribution for the cell under these operation conditions (insert to Fig. 7) exhibits behaviour corresponding to the water distribution scenario described above. At each voltage, the value of the HFR passes through a maximum and then decreases gradually as distance from gas inlet increases. The average HFR value is seen to be highest at the highest current density (cell voltage of 0.2 V), because of the depletion of water near the anode side of the Nafion^{TM} 117 membrane by electroosmotic drag [7]. The lowest average HFR is found at medium current densities (0.5 V), while it is somewhat higher than that at low current densities (0.7 V). The latter observation indicates the contribution of water generated within the cell to membrane hydration. At the air outlet, the segment high frequency resistance value is very similar to that commonly measured in smaller (5 cm^2) cells for Nafion^{TM} 117 membranes.

A further diagnostic tool was the ability to obtain complete polarization curves for individual segments, while the remaining cell segments operated at constant voltage (commonly 0.5 V). Figure 8 shows four polarization curves (scan from high to low voltage is shown) at four different locations along the flow channels; the operating conditions are the same as those described in Fig. 7. (The segment performance recorded in such polarization experiments is slightly worse at a given voltage, than that measured under steady state conditions, because of the direction of the voltage scan.) Comparison of the current and high frequency resistance against voltage curves (Fig. 8) confirms that the segments away from the air inlet are better hydrated, resulting in both lower membrane resistance and improved cathode catalytic performance. Finally, regarding the results described in Figs 7 and 8, it should be clear that such current distribution profiles are not necessarily the general rule in PEFCs. They are obviously generated by specific features of the cell and by specific operation conditions. Particularly, high flow of somewhat undersaturated air, combined with the thick ionomeric membrane employed, have resulted here in a relatively dry inlet region, in spite of the strong hydration

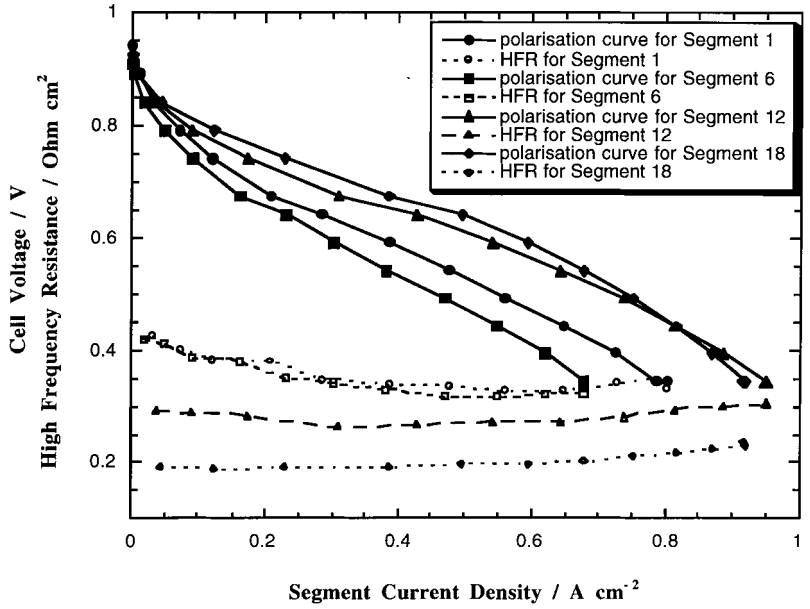

Fig. 8. Segment polarization and high frequency resistance curves comparing performance of segments 1 (air inlet), 6, 12 and 18 (air outlet). Hydrogen was humidified at 100 °C and passed through the cell at 0.71 min^{-1}, at a back pressure of 2.8 atm. Air was humidified at 80 °C and passed through the cell at 5.01 min^{-1}, at a back pressure of 2.8 atm. (See comment on actual humidification levels in caption for Fig. 7.)

of the hydrogen feed stream. This situation may possibly be avoided in a stack employing a thinner membrane and operated with saturated air at lower flow rates. Clearly, however, from the results presented, the segmented cell is effective in diagnosing the consequences of a specific combination of cell and operation conditions.

One of the primary reasons of establishing a method for measurement of current distribution in PEFCs is to better understand water management in larger cells and optimize cell humidification conditions. Current and high frequency resistance distributions in the cell were obtained at a cell voltage of 0.5 V for cathode humidification conditions (see Fig. 9) varying from dry air to air humidified at nominal 100 °C. In all experiments the anode gas was humidified at nominal 100 °C. Extremes in humidification conditions were chosen to highlight resulting

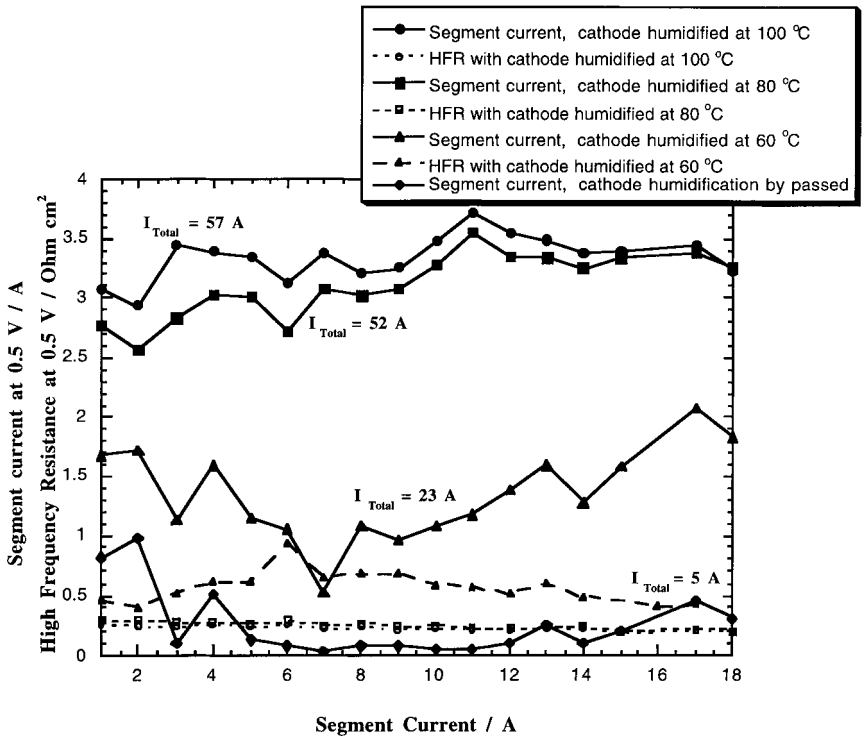

Fig. 9. Effect of varying cathode humidification conditions on the cell current and high frequency resistance distribution at a cell temperature of 80 °C. Hydrogen was humidified at 100 °C and passed through the cell at 0.71 min^{-1}, at a back pressure of 2.8 atm. Air was humidified at 60, 80 and 100 °C or by passed and passed through the cell at 5.01 min^{-1}, at a back pressure of 2.8 atm. (See comment on actual humidification levels in caption for Fig. 7.)

differences in cell current distributions. There is a substantial difference in the behaviour of the cell under these different humidification regimes. The best overall cell performance is achieved when air is humidified at nominal 100 °C, whereas dry air produced very poor cell performance in these experiments, as one would expect for such a relatively thick ionomeric membrane (Nafion^{TM} 117). The air stream in the flow channel appears to be insufficiently humidified until air humidification temperature is increased to nominal 100 °C. (Because of the limited effectiveness of gas humidification in our system (see experimental) water content for a nominal 100 °C humidifier temperature was only about 50% above saturation level for a cell temperature of 80 °C.) Under less vigorous humidification conditions, segment performance increases as distance from the air inlet increases, indicating internal humidification of the air increases performance. When the air stream is humidified at nominal 80 °C, internal humidification through the flow field means that later segments (i.e., segment numbers 14–18) perform as well as those externally humidified at nominal 100 °C. Therefore, water flux through the membrane is the same for the two different humidification conditions only at the outlet end of the cell. The minimum in current density distribution and maximum in high frequency resistance distribution observed progressing down the air flow stream are most clearly observed when the cathode is humidified at a nominal temperature of 60 °C (Fig. 9). Again, this severe cell drying noticeably takes place although the hydrogen feed stream is well humidified, but is most probably exacerbated under the specific experimental conditions employed here, that is, high air flow rates and a thick ionomeric membrane. It is highly likely, however, as these results suggest, that air stream humidification would be required in PEFCs to establish full hydration at the cathode at lower cell current densities, even under lower flows of air and with thinner cell membranes.

The effect of varying anode humidification on current and high frequency resistance distribution was subsequently investigated (Fig. 10). The best overall cell performance was again found when the anode was humidified at nominal 100 °C. When less aggressive humidification conditions were used, segment current was found to increase from hydrogen inlet to outlet (note: hydrogen inlet is plotted as segment 2 and outlet at segment 17). This is the same trend as observed when the cathode is poorly humidified, but wider distributions of membrane resistance and current density are seen. Apparently, when the anode is not sufficiently humidified, water generated at the cathode and passing through the membrane enables better hydration of the anode side of the membrane and of the anode catalyst down the flow channel. Again, the specific experimental conditions employed have an effect on the specific current distribution effects observed here with our segmented cell. The thick Nafion^{TM} 117 membrane exacerbates the effects of limited anode humidification, by limiting the rate of transport of cell generated water from the cathode to the anode. In addition, when hydrogen utilization approaches unity in

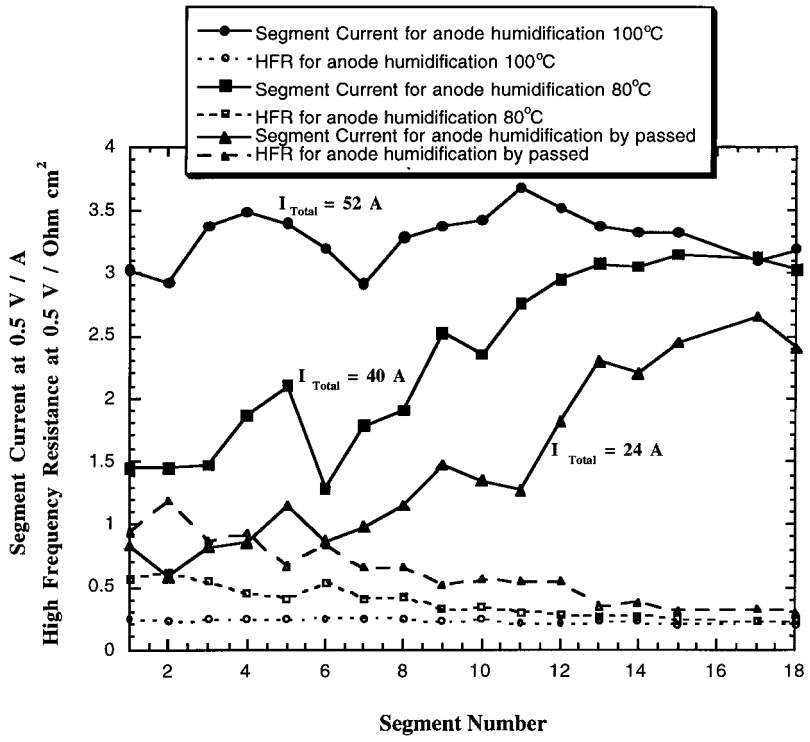

Fig. 10. Effect of varying anode humidification conditions on the cell current and high frequency resistance distribution at a cell temperature of 80 °C. Air was humidified at 80 °C and passed through the cell at 5.0 l min^{-1}, at a back pressure of 2.8 atm. Hydrogen was humidified at 80 and 100 °C or by passed and passed through the cell at 0.7 l min^{-1}, at a back pressure of 2.8 atm. (See comment on actual humidification levels in caption for Fig. 7.)

operation with neat hydrogen feed streams, water condensation could, in fact, take place down the flow channel. The anode could thus present quite different humidification requirements when cell and/or operation conditions are significantly changed.

A further important variable in achieving efficient fuel cell operation is operating at the minimum stoichiometric flow possible. Figure 11 shows the effect of changing the airflow rate (air stoichiometry). When air flow is less than three times stoichiometric flow, the current distribution profile indicates a loss in performance for segments at the end of the flow field (i.e., those nearest the air outlet), while segments at or near the air inlet see no change in performance. The high frequency resistance distributions have a similar form at all flow rates (see Fig. 11, insert), however, higher air flow rates produce higher resistance throughout the cell. This is probably the effect of more water being removed by the faster under saturated air stream. Polarization curves (Fig. 12) for the segment nearest air inlet (segment 1) show that the performance of this area of the cell is not affected by the air flow rate. In contrast, the performance of segment 18 nearest the air outlet, (Fig. 13) is greatly affected by air flow rate, so that limiting currents become apparent in the polarization curves at low flow rates. Figure 14 shows the polarization and high frequency resistance curves for four cell segments at an air flow rate of $0.61\,\mathrm{min}^{-1}$ (approximately 1.5 times stoichiometric flow). Progressing down the flow field smaller limiting currents are clearly observed as a result of limited transport of oxygen to the cathode catalyst layer, from a gas mixture depleted of the reactant gas component.

4. Conclusions

The printed circuit board cell fabrication approach described here has been found to be convenient and useful in the preparation of segmented electrodes and measurement of current distributions along the flow channel in PEFCs. This approach provides a useful tool for investigating different flow field designs and for optimizing utilization of the active electrode area with the most appropriate reactant stoichiometries and humidification conditions. In our current work, we limited investigations to a cell segmented into eighteen segments of relatively large area per segment, however the PCB technology allows fabrication of a larger number of segments of any given pattern. In fact, to better explore the local effects of water and reactant transport, a greater number of smaller segments may be preferable.

It was shown that the seven channel serpentine flow field employed can provide relatively uniform reactant and water supply throughout the active $100\,\mathrm{cm}^2$ electrode area, at the typical cell operating voltages of between 0.5 and 0.7 V. Optimum air

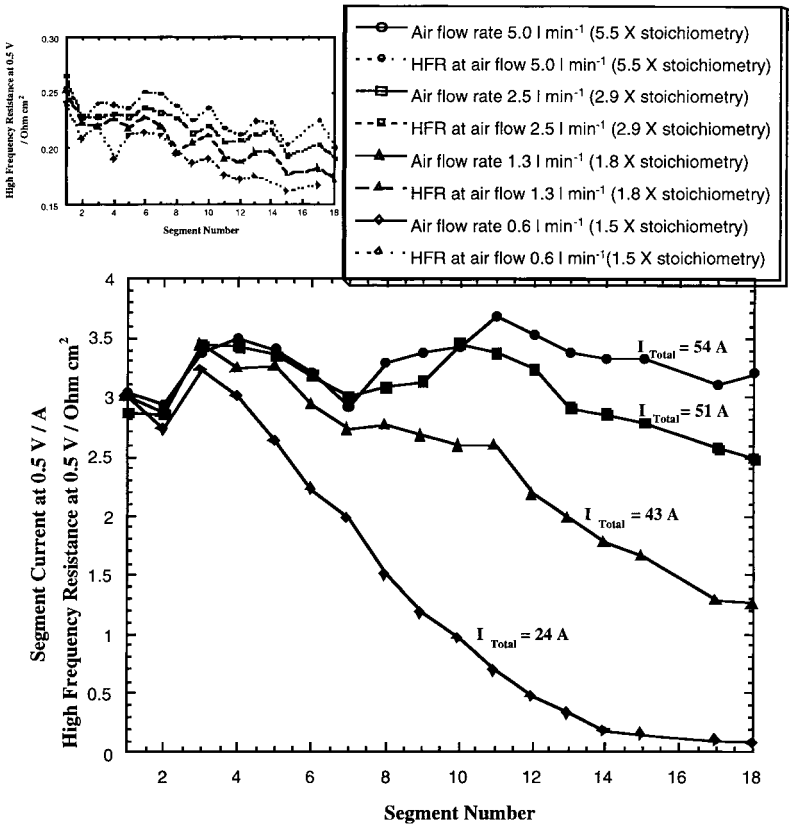

Fig. 11. Effect of varying cathode air flow rate (and hence air stoichiometry) on the cell current and high frequency resistance distribution at a cell temperature of 80 °C. Hydrogen was humidified at 100 °C and passed through the cell at $0.71\,\mathrm{min}^{-1}$, at a back pressure of 2.8 atm. Air was humidified at 80 °C and passed through the cell at flow rates between 5.0 and $0.61\,\mathrm{min}^{-1}$, at a back pressure of 2.8 atm. (See comment on actual humidification levels in caption for Fig. 7.)

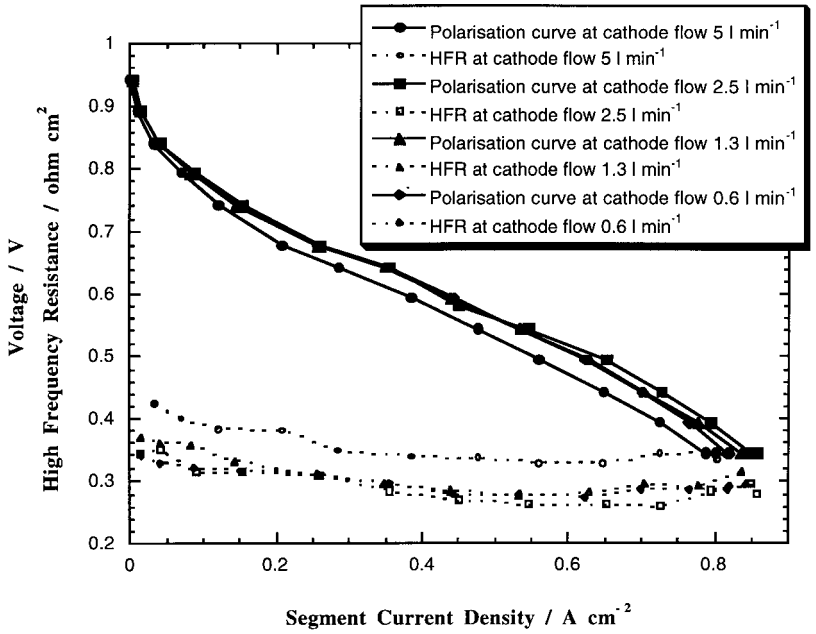

Fig. 12. Segment polarization and high frequency resistance curves comparing performance of segment 1, as a function of the air flow rate and stoichiometry. Hydrogen was humidified at 100 °C and passed through the cell at 0.7 l min^{-1}, at a back pressure of 2.8 atm. Air was humidified at 80 °C and passed through the cell at varying flow rates, at a back pressure of 2.8 atm. (See comment on actual humidification levels in caption for Fig. 7.)

cathode operating conditions at 2.8 atm with this flow field design, and using a Nafion^{TM} 117 membrane, were greater than 3 times stoichiometric flow rates and air humidification at nominal 100 °C (while the anode feed stream was kept well humidified). A typical trend found in the cell based on Nafion^{TM} 117 was increase in local performance from inlet to outlet due to lowered membrane resistance down the flow channel, thanks to improved humidification of membrane and catalyst layers down the channel by internal generation of water. This trend is amplified when the air feed stream is undersaturated, particularly if the flow rate is high. The trend is reversed at low stoichiometric flows of air, when effects of lowered concentrations of oxygen down the flow channel overshadow the effects of the increase in membrane conductivity.

Cell operation conditions chosen here for initial tests of this new type of segmented cell, are certainly not optimized from PEFC stack technology perspective, in terms of either gas pressures, flow rates (particularly fuel flow rates) or specific cell compo-

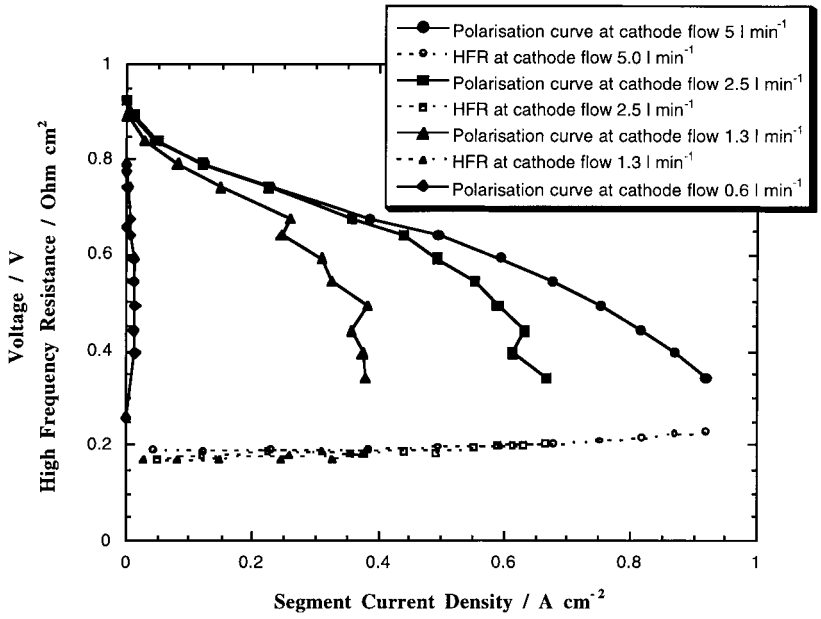

Fig. 13. Segment polarization and high frequency resistance curves comparing performance of segment 18, as a function of the air flow rate and stoichiometry. Hydrogen was humidified at 100 °C and passed through the cell at 0.7 l min^{-1}, at a back pressure of 2.8 atm. Air was humidified at 80 °C and passed through the cell at varying flow rates, at a back pressure of 2.8 atm. (See comment on actual humidification levels in caption for Fig. 7.)

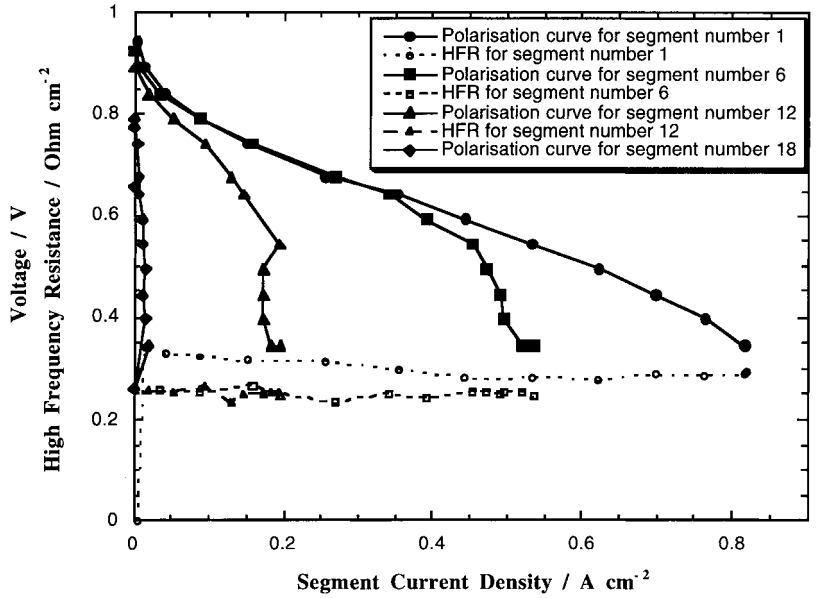

Fig. 14. Segment polarization and high frequency resistance curves comparing performance of segments 1, 6, 12 and 18 at 1.5 × air stoichiometry, in a cell containing a seven channel serpentine flow field. Hydrogen was humidified at 100 °C and passed through the cell at 0.71 min^{-1}, at a back pressure of 2.8 atm. Air was humidified at 80 °C and passed through the cell at 0.61 min^{-1}, at a back pressure of 2.8 atm. (See comment on actual humidification levels in caption for Fig. 7.)

nents. The exact nature/values of all of those parameters would, in any case, depend to significant degree on a specific stack design and application. Conditions were chosen here primarily to highlight the potential of this cell for effective cell diagnostics. We report in a subsequent publication on more observations with this type of segmented cell, collected for cells employing different flow fields and MEAs based on thinner membranes.

Acknowledgements

Support by US DOE, Office of Advanced Automotive Technology (OAAT) is gratefully acknowledged.

References

[1] D. Pletcher and F. C. Walsh, 'Industrial Electrochemistry', 2nd edn, Blackie (1990).
[2] A. Stock and F. Coeuret, *Electrochim. Acta.* **22** (1977) 1155.
[3] L. R. Czarnetzki and L. J. J. Janssen, *J. Appl. Electrochem.* **19** (1989) 630.
[4] W. W. Folke, *Electrochimi. Acta.* **28** (1983) 1137.
[5] C. J. Brown, D. Pletcher, F. C. Walsh, J. K. Hammond and D. Robinson, *J. Appl. Electrochem.* **22** (1992) 613.
[6] P. Adcock, P. Mitchell and J. Moore, Poster P1-30 of the Fuel Cell Seminar, San Diego, CA.
[7] T. E. Springer, T. A. Zawodzinski, and S. Gottesfeld, *J. Electrochem. Soc.* **138** (1991) 2334.
[8] D. M. Bernardi and M. W. Verbrugge, *AIChE J.* **37** (1991) 1151.
[9] T. V. Nguyen and R. E. White, *J. Electrochem. Soc.* **140** (1993) 2178.
[10] T. F. Fuller and J. Newman, *ibid.* **140** (1993) 1218.
[11] S. J. C. Cleghorn, C. R. Derouin, M. S. Wilson and S. Gottesfeld, San Antonio Meeting, Electrochemical Society (1996), Abstract 798.
[12] F. A. Uribe, T. E. Springer and S. Gottesfeld, *J. Electrochem. Soc.* **139** (1992) 765.
[13] T. E. Springer, M. S. Wilson and S. Gottesfeld, *ibid.* **140** (1993) 3513.
[14] C. Zawodzinski, M. S. Wilson and S. Gottesfeld, in 'Proton Conducting Membrane Fuel Cells I' (edited by S. Gottesfeld, G. Halpert and A. Landgrebe), The Electrochemical Society Proceedings Series, **95-23**, (1995), p. 57.
[15] M. S. Wilson, J. A. Valerio and S. Gottesfeld, *Electrochim. Acta.* **40** (1995) 355.